

Experimental study of mixed-mode crack propagation in RC beams without stirrups

J. R. Carmona, G. Ruiz & J. R. del Viso

E.T.S. de Ingenieros de Caminos, Canales y Puertos, Universidad de Castilla-La Mancha, Spain

ABSTRACT: This paper presents the results of a very recent experimental research program aimed at investigating mixed-mode fracture of longitudinally reinforced concrete beams. The tests were designed so that only one single mixed-mode crack generates and propagates through the specimen, as opposed to the usual dense crack pattern found in most of the tests in scientific literature. The specimens were three-point-bend beams of three different sizes. They were notched asymmetrically and reinforced with various ratios of longitudinal reinforcement. These experiments may help to understand the mechanisms of mixed-mode crack propagation in longitudinally reinforced concrete elements. Finally an analytical model based on the experimental results model is presented to analyze size effect and hyper-strength in this kind of elements.

1 INTRODUCTION

This paper presents some very recent results of an experimental program aimed at disclosing some aspects of the propagation of mixed-mode cracks through longitudinally reinforced concrete elements and its consequences. Specifically, the program was designed to investigate the influence of the size of the specimen and of reinforcement detailing on mixed-mode crack propagation. This research is an extension of previous works on the nucleation and propagation of mode I cracks in reinforced concrete (Ruiz et al., 1998; Ruiz and Carmona, 2006). By focusing on mixed-mode cracks we aim at completing the study of the generation and development of the different types of cracks that may appear in longitudinally reinforced concrete beams.

In reinforced concrete, mixed-mode crack propagation is mainly addressed from a technological standpoint. The dense crack pattern that results from the usual reinforcement detailing and element geometry may somehow make it difficult to induce direct relations between causes and effects. That is why we focus on the propagation of one single mixed-mode crack. Of course, there are some other excellent studies with common points with our methodology. They addressed problems related to the shear resistance of reinforced elements, like the study on failure by diagonal tension performed by Bažant and Kazemi (Bažant and Kazemi, 1991), or the work by Kim and White (Kim and White, 1999) on the generation of

shear-damaged in reinforced concrete.

The article is organized as follows. An outline of the experimental program is given in Section 2. In Section 3 we describe the characterization tests performed on the materials used to make the reinforced beams. Section 4 deals with the experimental set-up for the mixed-mode tests. The experimental results are presented and discussed in Section 5. Section 6 include a simple analysis of size effect in reinforced notched concrete beams. Finally, in Section 7 some conclusions are extracted.

2 OVERVIEW OF THE EXPERIMENTAL PROGRAM

The program was designed to study the propagation of mixed-mode cracks through reinforced concrete. Specifically, we wanted to disclose the influence of the amount of reinforcement and specimen size on the crack propagation. We also intended to analyze the variations in the crack pattern and in the mechanical behavior due to the size of the specimens. In addition, the program had to provide an exhaustive material characterization to allow a complete interpretation of the test results.

With these intentions in mind, we chose the beam sketched in Figure 1 as a convenient specimen for this research. Our choice revisits the geometry tested by Jenq and Shah to study mixed-mode crack propagation in plain concrete (Jenq and Shah, 1988). It is a notched beam that exhibits a single mixed-mode

crack when subjected to bending at three points. In their work, Jenq and Shah provide plenty of insights on the generation and propagation of the crack which are of use here. We reinforce the beams with several ratios of longitudinal ($\rho_l = \frac{A_l}{BD}$, being A_l the area of the cross section of the longitudinal reinforcing bars, B the beam width and D the beam depth). The reinforcement provokes changes in the orientation of the main crack and in the global mechanical response, but the presence of a notch avoids a dense crack pattern that would blur our perception of such changes. At most, some reinforcement configurations generate a secondary flexural crack at midspan that competes with the one that starts from the notch tip.

Regarding the size of the beams, we wanted even the largest beams to be reasonably easy to handle and test. At the same time, the behavior of the laboratory beams should be representative of the behavior of beams of a normal size made of ordinary concrete. In order to fulfill both requirements, Hillerborg's brittleness number β_H (Bažant and Planas, 1998) was used as the comparison parameter. It is defined as the ratio between the size of the beams—represented by their depth D —and the characteristic length of the concrete, ℓ_{ch} (Pettersson, 1981), i.e.:

$$\beta_H = \frac{D}{\ell_{ch}}, \text{ where } \ell_{ch} = \frac{E_c G_F}{f_t^2}, \quad (1)$$

E_c is the elastic modulus, G_F the fracture energy and f_t the tensile strength. As a first approximation, two geometrically similar structures display a similar fracture behavior if their brittleness numbers are equal. According to this, a relatively brittle micro-concrete was selected with a characteristic length of approximately $\ell_{ch} = 90$ mm (the details of the micro-concrete are given in the next section), while the beams were made to be 75, 150 and 300 mm in depth. Since ℓ_{ch} of ordinary concrete is 300 mm on average, our 150 mm depth laboratory beams are expected to simulate the behavior of ordinary concrete beams 500 mm in depth, which is considered as a reasonable size for the study.

The dimensions were scaled to the beam depth D , please see Figure 1. We made small (S, $D = 75$ mm), medium (M, 150 mm) and large (L, 300 mm) specimens reinforced with several ratios of longitudinal reinforcement. The beam width is in all cases equal to 50 mm. Each specimen was named by a letter indicating the size (S, M or L) and one figure indicating the number of bars used for the reinforcement. For example, L2 names a large beam with two longitudinal bars. We performed at least two tests for each type of beam.

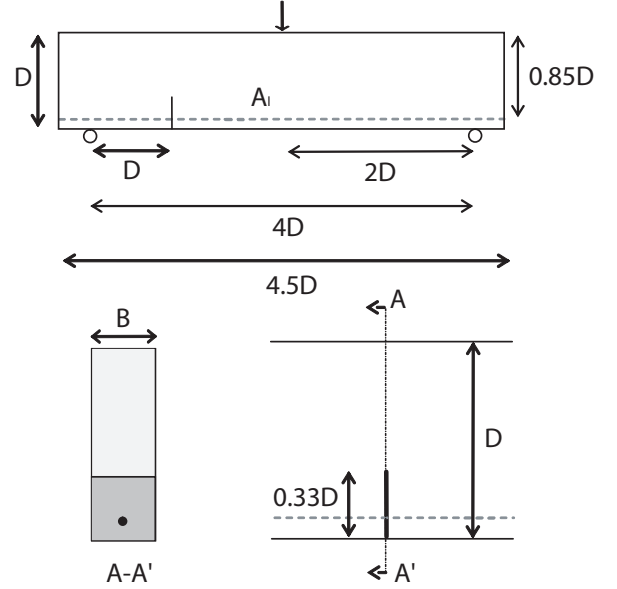


Figure 1: Beam Geometry.

Table 1: Micro-concrete mechanical properties.

	f_c ^(a) MPa	f_{ts} ^(b) MPa	E_c GPa	G_F N/m	ℓ_{ch} mm
<i>mean</i>	36.3	3.8	28.3	43.4	86.8
<i>std. dev.</i>	1.9	0.3	2.7	5.8	-

^(a) Cylinder, compression tests.

^(b) Cylinder, splitting tests.

3 MATERIALS CHARACTERIZATION

3.1 Micro-concrete

A single micro-concrete mix was used throughout the experimentation, made with a lime aggregate of 5 mm maximum size and ASTM type II/A cement. The mix proportions by weight were 3.2 : 0.45 : 1 (aggregate : water : cement). We made characterization specimens out of all batches.

Compression tests were carried out according to ASTM C 39 and C 469 on 75×150 mm cylinders (diameter \times height). Brazilian tests were also carried out on these kind of cylinders following the procedures recommended by ASTM C 496. Stable three-point bend tests on $75 \times 50 \times 337.5$ mm notched beams were carried out to obtain the fracture properties of concrete. We followed the procedures devised by Elices, Guinea and Planas (that are minutely explained in (Bažant and Planas, 1998)). Particularly, during the tests the beams rested on anti-torsion devices. They consist of two rigid-steel semi-cylinders laid on two supports permitting rotation out of the plane of the beam and rolling along the longitudinal axis of the beam with negligible friction. Table 1 shows the mechanical parameters of the micro-concrete determined in the various characterization

Table 2: Steel mechanical properties.

E_s	$f_{y,0.2}$	f_u	ε_u
GPa	MPa	MPa	%
174	563	632	4.6

and control tests.

3.2 Steel

For the beam dimensions selected and the desired steel ratios, the diameter of the steel bars had to be smaller than that of standard rebars, so commercial ribbed wires with a nominal diameter of 2.5 mm were used as reinforcing bars. Table 2 shows the mechanical properties of the ribbed wires. The elastic modulus E_s , the ultimate strength f_u , the 0.2% offset yield strength $f_{y,0.2}$, and the ultimate strain ε_u . The nominal value of the diameter was used to calculate the stress-related parameters in Table 2.

The ultimate strain in ribbed bars is considerably lower than in mild steel bars, due to the defects in the material resulting from the ribbing process.

3.3 Steel-concrete interface

Pullout tests were carried out by pulling the wire at a constant displacement rate while keeping the concrete surface compressed against a steel plate. Figure 2a sketches the pull out specimen, a prism of $50 \times 50 \times 75$ mm with a wire embedded along its longitudinal axis. The bonded length was 25mm (=10 \times nominal diameter of the bars) to allow a constant shear stress at the interface of the reinforcement wires (Losberg and Olsson, 1979; RILEM/CEB/FIP, 1970). The relative slip between the wire and the concrete surfaces was measured at the bottom end. The tests were carried out at a constant displacement rate of $2\mu\text{m/s}$. Figure 2b, shows the upper and lower limit of the bond-slip curves. The bond strength τ_c deduced from these tests was 6.4 ± 1.8 MPa. The scatter is over 30%, typical for this kind of test.

4 MIXED-MODE TESTS

As we already described in Section 2, the specimens for the mixed-mode tests were notched beams reinforced with longitudinal bars. Figure 1 sketches the geometry and reinforcement detailing of the beams;

All the beams were supported and tested in three-point bending tests, as illustrated in Figure 1. During the tests the beams rested on anti-torsion supports like the ones used to measure G_F (see Section 3.1). For loading, a hydraulic servo-controlled test system was employed. The test were performed in position-control. We ensured that the evolution of the crack-ing process was very slow. The maximum load was achieved for each size within about 60-80-min. Each

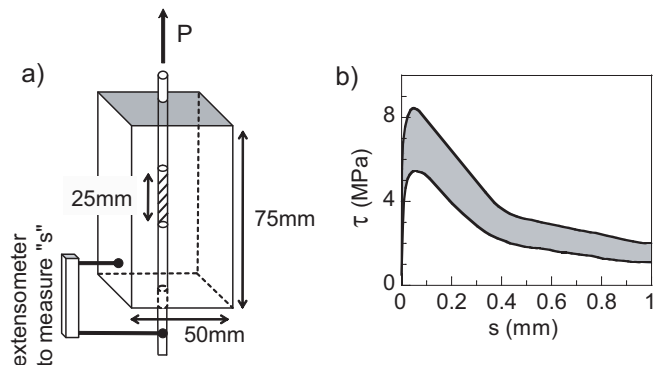


Figure 2: (a) Pull-out specimen to obtain steel-concrete interface properties; (b) upper and lower limit of the $\tau - s$ curves.

complete test had a duration of 120-140 min.

The load, P , and the displacement under the load point, δ , were continually monitored and recorded. We also used a resistive extensometer centered on the tensioned face of the beam at the mouth of the notch to measure the crack opening displacement, c_{MOD} , in all the tests. In order to complete the experimental information, we also drew the crack pattern resulting from each test copying it directly from both sides of beam.

5 DISCUSSION

Figure 3 shows experimental $P-\delta$ and $P-c_{MOD}$ curves. Plain beams, as a limit case of this category of beams, are also considered in the figures. In this kind of beams, the reinforcing bars are far from the tip of the notch. The crack starting from the notch should behave like a crack that has already crossed the flexural reinforcement layer and goes on progressing under mixed-mode conditions. To facilitate the comparison between $P-\delta$ curves corresponding to the same kind of beams, the initial slope of the curves is corrected to the theoretical value obtained from finite element calculations. Different experimental initial slopes in a $P-\delta$ curve are usual even for the same kind of beams and the same set-up. This is due to the sensitivity of the elastic flexibility of the beam to the boundary conditions in the application of a concentrated load (Planas et al., 1992).

The crack propagation process can be understood with the help of Figures 4 and 5. They show the evolution of the crack related to the $P-\delta$ and the $P-c_{MOD}$ curves for a L4 specimen (Fig. 4) and L8 beam (Fig. 5). Please remember that L4 is a large beam — $D=300\text{mm}$ — reinforced with 4 longitudinal ribbed bars —the reinforcement ratio is 0.13%—. Figure 4a shows a picture of the specimen after being tested. The crack trajectory was digitalized and sketched in Figure 4b. The marks and figures on the sketch refer

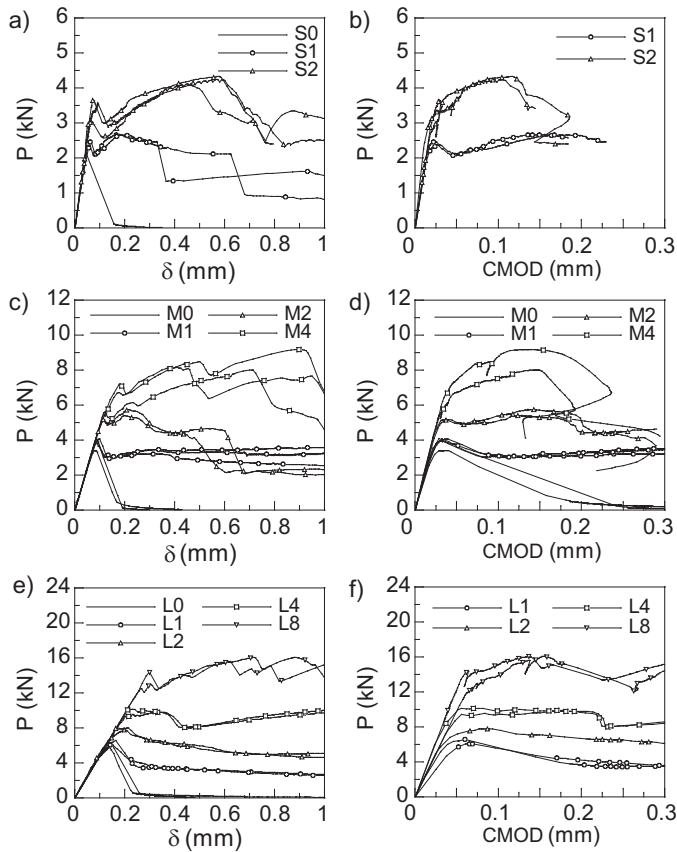


Figure 3: Experimental results given by beams with various ratios of longitudinal bars: (a) P - δ curves of the small beams; (b) P -CMOD curves of the small beams; (c) P - δ curves of the medium beams; (d) P -CMOD curves of the medium beams; (e) P - δ curves of the large beams; (f) P -CMOD curves of the large beams.

to the corresponding points in the P - δ and P -CMOD curves (Figs. 4c and d respectively) and to the load in kN that the beam was standing when the crack tip reached that position. Thus, Figure 4 contains all the experimental information recorded during the test of beam L4-7-2 (the last two numbers indicate that the beam was the second of its kind taken from batch number 7).

The behavior of the beam is almost linear up to the cracking load, P_c , which is assigned the label A in Figures 4b-d. From then on the crack propagates in a slow and stable manner until its tip reaches the point labelled as C. Please note that the propagation between A and C implies almost no increase in the external load. The displacement δ in C is twice the elastic δ that corresponds to A, whereas the crack opening in C is four times longer that the one in A. From C the crack goes on propagating stably towards D, but the curves show that the type of propagation has changed. Indeed, the crack length between C and D equals the growth between A and C but the loads drop from 9.8 to 8.1 kN and, strikingly, the crack growth is not associated to any δ neither CMOD increase. The change in the nature of the propagation can also be

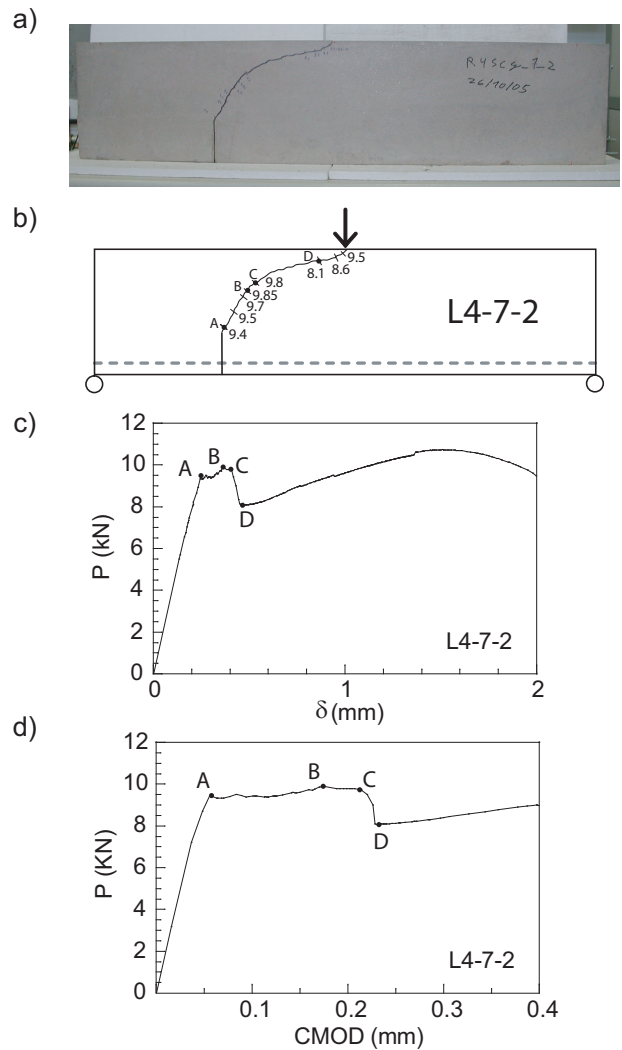


Figure 4: Crack propagation in the specimen L4-7-2: (a) photograph; (b) crack trajectory (the marks denote the extent of cracking at the given loads in kN); (c) P - δ curve; (d) P -CMOD curve.

noticed by a deviation in the crack trajectory (Fig. 4b). In reinforced concrete technology the behavior just described is referred to as failure due to diagonal tension. It implies a redistribution of the way of resisting shear within the beam. Part of the load carried by the concrete ligament is transferred to the steel bars and that is why the beam recovers some strength at D. From then on the crack goes on propagating slowly towards the loading point. Most of the shear is withstood by the bars that sew the crack. Depending on the ratio and cover of longitudinal reinforcement and on the geometry of the beam, the concrete around the bars may not be strong enough to resist the shear transferred by the reinforcement. In such cases the bars provoke the generation of a longitudinal crack at the level of the reinforcement, which implies a sudden drop in the load capacity.

Figure 5 provides additional insights on the propagation process, since a L8 beam is reinforced with 8 longitudinal bars, thus doubling the reinforcement

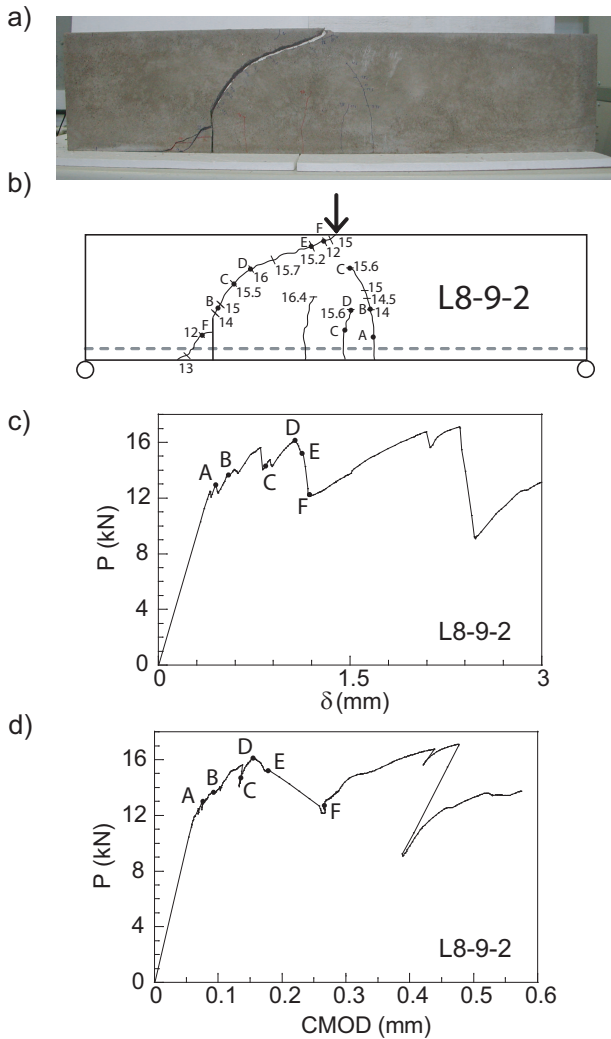


Figure 5: Crack propagation in the specimen L8-9-2: (a) photograph; (b) crack trajectory (the marks denote the extent of cracking at the given loads in kN); (c) P - δ curve; (d) P -CMOD curve.

ratio. Interestingly, the increase in the reinforcement ratio provokes the generation of flexural cracks that initially grow faster than the mixed-mode crack, as the stretch AB in Figure 5b shows. From B to D flexural cracks compete with the mixed-mode crack generated at the notch tip, the propagation being slow and stable. At this point, like in the previous case, the nature of the propagation changes. Figure 5b-d show that the mixed-mode crack grows rapidly in a stable way (stretch DE) whereas the flexural cracks arrest; likewise, points D and E are very close both in the P - δ and P -CMOD curves. There has been a redistribution of the shear carrying capacity from the concrete ligament to the steel bars. The concrete that surrounds the reinforcement is not able to stand the load transmitted by the bars and then there starts a longitudinal crack at the reinforcement level. The big jump between E and F in the CMOD indicates the opening of this new crack.

The trajectory of the crack is sensitive to the pres-

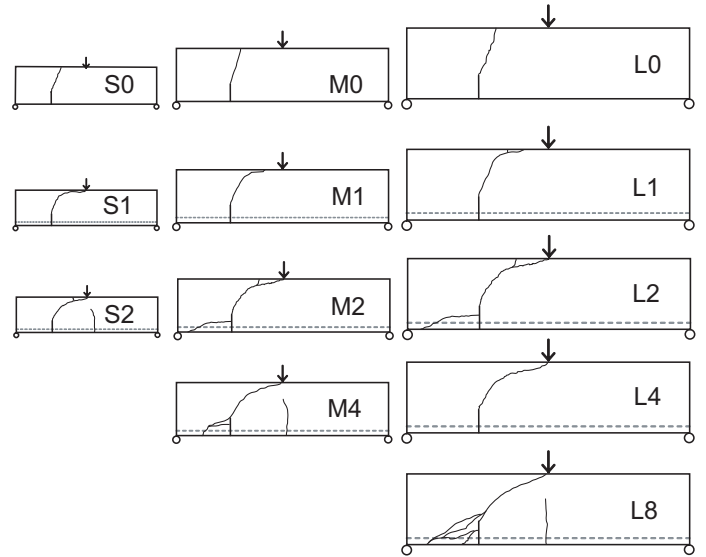


Figure 6: Crack pattern observed in beams with various ratios of longitudinal bars and no inclined bars.

ence and amount of flexural reinforcement, as Figure 6 clearly shows. The sketches to represent the crack pattern of the beams of different size do not keep the proportionality between the actual beams, which is 1 : 2 : 4. To facilitate the comparison we represent the sketches scaled following the ratio 1 : 1.5 : 2. Although two tests have been done per each beam type, we have selected only one of the resulting patterns to represent the beam type, since crack patterns for the same beam type are quite similar in all cases. The angle at which the crack starts propagating is almost independent from the number of bars, but as the reinforcement ratio increases, the crack gets inclined so as to reach the loading point. In this case, crack trajectories for different beam sizes are alike. All the beams broke due to the propagation of the mixed-mode crack.

The influence of the reinforcement ratio in the cracking load is analyzed in Figures 7a and b. They represent the cracking load in a nondimensional way versus the reinforcement ratio. The geometry and reinforcement arrangement in these beams facilitate that the bars work as soon as the beam starts to be loaded, which provokes a hyper-strength associated to the ratio of reinforcement. For the ratios considered, a linear relation between reinforcement ratio and cracking load fits very well the test results (please, note that the Pearson's correlation coefficient, R in Figures 7a and b is very close to 1).

Figure 7c shows the cracking load against the size of the beam in a non-dimensional form. Plain beam results and the Bažant's law (Bažant, 1984) fitted to these results are also plotted to facilitate the comparison. As reinforcement ratio increases, size effect is less noticeable.

Figure 7d plots the maximum load (at diagonal ten-

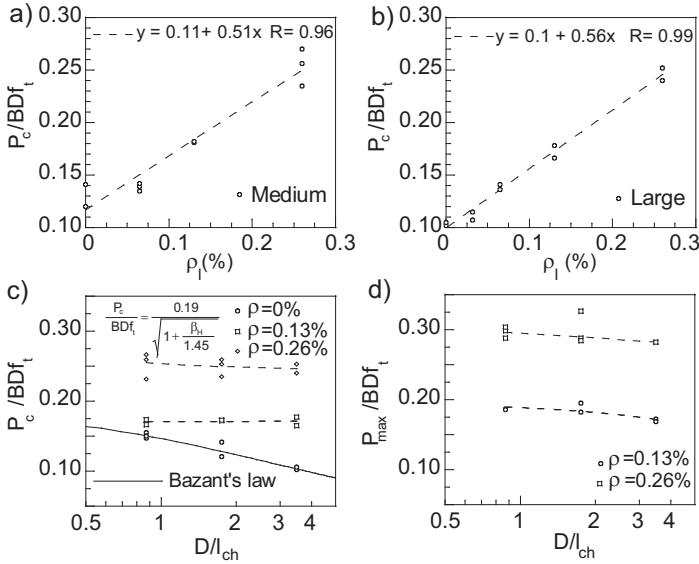


Figure 7: (a) Cracking strength versus reinforcement ratio for the medium beams; (b) cracking strength versus reinforcement ratio for the large beams; (c) cracking strength versus size; (d) maximum strength versus size.

sion failure), P_{max} , versus size in a nondimensional form. The strength decreases with size in a smoother way than for Bažant's law, that is, than for plain beams.

6 SIMPLE MODEL TO EXPLAIN SIZE EFFECT AND HYPER STRENGTH

We observe in Figures 3 and 7 a hyper-strength effect in cracking and maximum load due to the reinforcement action. According to (Ruiz, 2001) the cracking load, P_c , is a function, apart from beam geometry and boundary conditions, of concrete properties, element size and steel location and properties, including the bond-slip behavior of the steel-concrete interface. If reinforcement has reached its yield strength f_y , we can write:

$$P_c = f\left(\frac{D}{l_{ch}}, \frac{c}{l_{ch}}, \rho, \eta, \frac{f_y}{f_t}\right) \quad (2)$$

Where D is the depth of the beam, c is the length of the concrete cover and η is a nondimensional parameter that represents the strength of the interface (Ruiz, 2001). In this investigation only the reinforcement ratio and the size of the element are varied. So, we are going to consider as constants the rest of the parameters and thus Eq. 2 can be rewritten as:

$$P_c = f\left(\frac{D}{l_{ch}}, \rho, \frac{f_y}{f_t}\right) \quad (3)$$

To determine a simple expression to evaluate P_0 , we can decompose the load capacity of the beam in two terms. The first one represents the load stood by

the plain concrete. The second one includes the hyper-strength attributable to the presence of longitudinal reinforcement. Thus we can write:

$$P_c = P_0 + \Delta P \quad (4)$$

where P_c is the part on the load due to plain concrete and ΔP is the hyper-strength.

For the sake of simplicity, concrete carrying capacity is represented according to linear elastic fracture mechanics, the simplest fracture hypothesis. We can write:

$$\sigma_0 = \frac{P_0}{BD} = K_0 \beta_H^{-\frac{1}{2}} f_t \quad (5)$$

Where K_0 is a dimensionless constant for scaled plain beams, and β_H is the Hillerborg's brittleness number as defined in Eq. 1. The exponent $-\frac{1}{2}$ represents the strongest possible size effect. Applicability of such size effect to shear fracture was first analyzed in a pioneering study by Reinhardt (Reinhardt, 1981). It must be emphasized that Eq. 5 only wants to catch a trend of the actual behavior. Concrete response could be modelled with other expressions like Bažant's law (Bažant, 1984) or using another exponent like $-\frac{1}{4}$ (Hillerborg and Gustafsson, 1988).

ΔP in Eq. 4 can be considered as a function of the beam geometry, the position and mechanical properties of the steel rebars and of the bond-slip behavior of the steel-concrete interface. In our experimental program we have used a very low reinforcement ratio and the steel was most of the times yielded at the cracking load. We derived a linear relation between the hyper-strength and the longitudinal reinforcement ratio, based in the results showed in Figures 7a and b.

$$\sigma_\Delta = \frac{\Delta P}{BD} = K_\Delta \rho f_y \quad (6)$$

where K_Δ is another dimensionless constant provided the beams keep the same proportions and reinforcement ratio. The cracking strength can be rewritten as:

$$\frac{P_c}{BD} = \sigma_c = \sigma_0 + \sigma_\Delta = K_0 \beta_H^{-\frac{1}{2}} f_t + K_\Delta \rho f_y, \quad (7)$$

which can be expressed in a non-dimensional fashion as:

$$\frac{P_c}{BDf_t} = \frac{\sigma_c}{f_t} = K_0 \beta_H^{-\frac{1}{2}} + K_\Delta \rho \frac{f_y}{f_t} \quad (8)$$

Applicability of Eqs. 7 and 8 requires not only that the beams are scaled to each other, but also that the shape of the cracks be similar. In our case the crack patterns are very similar for the cracking load, as we showed in section 5.

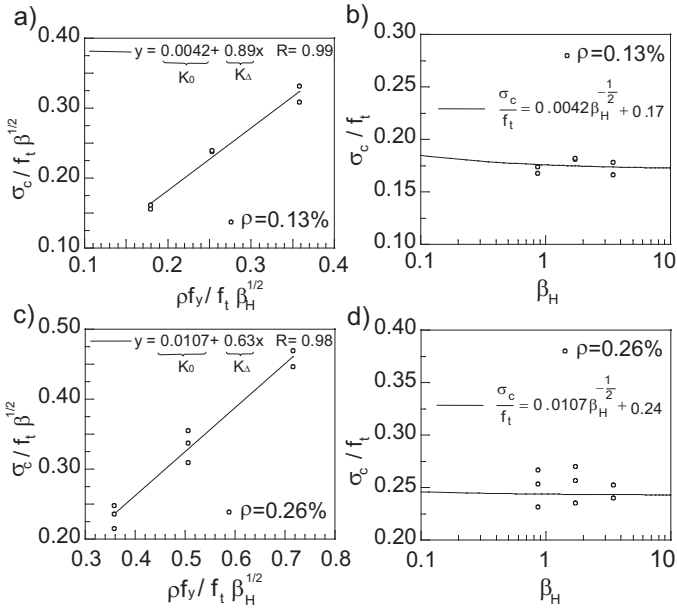


Figure 8: Size effect plots for cracking load: (a) results for the regression to calibrate K_0 and K_Δ coefficients for $\rho=0.13\%$; (b) size effect law for $\rho=0.13\%$; (c) results for the regression to calibrate K_0 and K_Δ coefficients for $\rho = 0.26\%$; (d) size effect law for $\rho=0.26\%$.

Figures 8a and c show the linear regression made with some of test results to get the constants K_0 and K_Δ . Figures 8b and d show tests results compared to the obtained size effect law. It may be pointed out that in notched reinforced concrete beams size effect tends to disappear when $D \rightarrow \infty$. The nominal shear strength converges to a value different from zero, which is a function on steel properties. Further analysis would be necessary to evaluate the influence of the mechanical behavior of the steel-concrete interface and of the geometry of the beam.

In reinforced concrete elements, the largest crack at maximum load has the same effect as the notches in fracture specimens. If we consider that diagonal tension failure is caused by fracture propagation and maximum load is attained only after a large fracture growth (and not at fracture initiation), then Eq. 7 will be susceptible to represent the ultimate strength at failure by diagonal tension. Test results available in the literature show that for diagonal tension failure, the LFM asymptote of slope $-1/2$ fits results better than a horizontal asymptote. This means that shear failure of beams is predominantly brittle (Bažant and Yu, 2005a; Bažant and Yu, 2005b) and so the hypothesis made in Eq. 5 can be considered accurate enough for our proposal.

To apply Eq. 7 to analyze diagonal tension failure we have to make some additional hypothesis. The first one is that the main crack in similar beams of various sizes has to be geometrically similar. This is a reasonable assumption having in mind our results, as it is observed in Figure 6 for $\rho=0.13\%$ and $\rho=0.26\%$. The

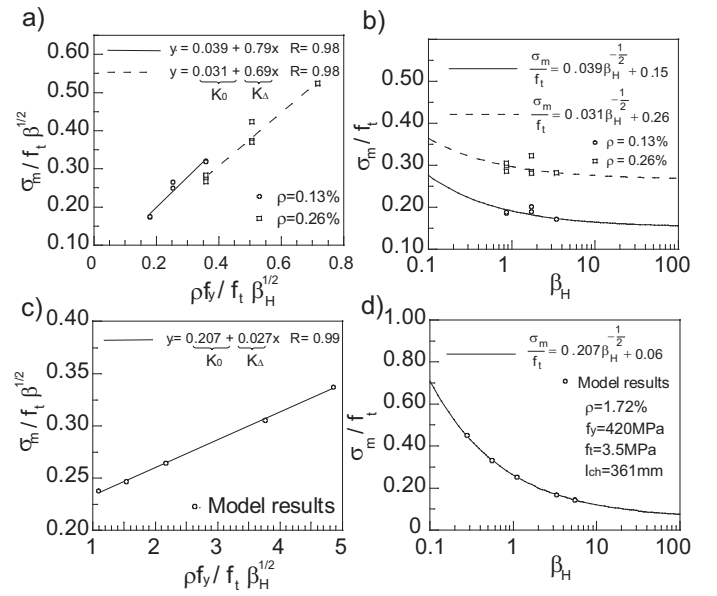


Figure 9: Size effect plots for maximum load: (a) results for the regression to calibrate K_0 and K_Δ coefficients, $\rho = 0.13\%$ and $\rho = 0.26\%$; (b) size effect law for $\rho = 0.13\%$ and $\rho = 0.26\%$; (c) results for the regression to calibrate K_0 and K_Δ coefficients for Ožbolt and Elige-hausen results; (d) size effect law for Ožbolt and Elige-hausen results.

second hypothesis is that steel stress in similar structures of various sizes at failure have to be similar. In beams without any notch diagonal tension failure occurs when the steel is still in the elastic range. In Eq. 6 we consider that the steel yielded because this is what happens in our tests due to the low reinforcement ratio. In un-notched beams f_y has to be changed by σ_s , steel tension at failure.

Figure 9a shows the linear regression made to get K_0 and K_Δ constants for the beams that failed by diagonal tension. Figure 9b shows the tests results against the obtained law. We have followed the same procedure with results obtained by Ožbolt and Elige-hausen (Ožbolt and Elige-hausen, 1997) (Figs. 9c and d). We selected these results due to the wide size range that they cover (0.1-2.0 m) and the accuracy obtained from their model. The size effect model that we propose fits their results quite well, which proves that the model catches the trends of the response. Summarizing, tests results indicate that the strength tends to converge to a constant value different from zero. The proposed model follows this tendency, based on experimental observations. It can be of use to develop recommendations on shear reinforcement requirements.

7 CONCLUSIONS

This article presents very recent experimental results on the propagation of mixed-mode cracks through reinforced concrete. The tests were designed so that

only one single mixed mode crack generates and propagates through the specimen, as opposed to the usual dense crack pattern found in most of the tests in scientific literature. The specimens were three-point-bend beams with an asymmetrical notch of three different sizes reinforced with various ratios of longitudinal (flexural) reinforcement.

The cracking load of beams was very sensitive to the amount of reinforcement and the crack propagated towards the point where the load was applied. Another observation is that after a large crack progress the final stretch of the crack propagation induced a sudden drop in the carrying capacity of the beam, similar to the so-called diagonal tension failure. Also the effect of the size of the beams is noticeable in our tests. On the one hand, large beams resisted less load in terms of stress. On the other hand the larger the beam, the more leaned towards the load point the crack trajectory was. These experimental results can be used profitably for modeling the behavior of mixed mode crack propagation on reinforced concrete beams.

Finally, the size effect in both cracking and maximum load (at the failure by diagonal tension) is accurately described by a simple model. It discloses the influence of the ratio of longitudinal reinforcement on the hyper-strength and subsequently, can enlighten code developers on updating recommendations for shear reinforcement provisions.

ACKNOWLEDGEMENTS

The authors gratefully acknowledge financial support for this research provided by the *Ministerio de Fomento*, Spain, under grant BOE305/2003, and the *Junta de Comunidades de Castilla -La Mancha*, Spain, under grant PAI05-028.

REFERENCES

- Bažant, Z. P. (1984). Size effect in blunt fracture: Concrete, rock, metal. *Journal of Engineering Mechanics-ASCE*, 110:518–535.
- Bažant, Z. P. and Kazemi, M. P. (1991). Size effect in diagonal shear failure. *ACI Structural Journal*, 88(3):268–276.
- Bažant, Z. P. and Planas, J. (1998). *Fracture Size Effect in Concrete and Other Quasibrittle Materials*. CRC Press, Boca Raton.
- Bažant, Z. P. and Yu, Q. (2005a). Designing against size effect on shear strength of reinforced concrete beams without stirrups: I. Formulation. *Journal of Structural Engineering-ASCE*, 131(12):1877–1885.
- Bažant, Z. P. and Yu, Q. (2005b). Designing against size effect on shear strength of reinforced concrete beams without stirrups: II. Verification and calibration. *Journal of Structural Engineering-ASCE*, 131(12):1886–1897.
- Hillerborg, A. and Gustafsson, P. J. (1988). Sensitivity in shear strength of longitudinally reinforced concrete beams to fracture energy of concrete. *ACI Structural Journal*, 85(3):286–294.
- Jenq, Y. S. and Shah, S. P. (1988). Mixed mode fracture of concrete. *International Journal of Fracture*, 38:123–142.
- Kim, W. and White, R. N. (1999). Shear-critical cracking in slender reinforced concrete beams. *ACI Structural Journal*, 96(5):757–765.
- Losberg, A. and Olsson, P. A. (1979). Bond failure of deformed reinforcing bars based on the longitudinal splitting effect of the bars. *ACI Journal*, 76(1):5–17.
- Ožbolt, J. and Eligehausen, R. (1997). Size effects in concrete and RC structures - Diagonal shear and bending. In *CEB Bulletin d'Information n 137 - Concrete Tension and Size Effects*, pages 103–145, Lausanne, Switzerland. Comite Euro-International du Béton (CEB).
- Petersson, P. E. (1981). *Crack Growth and Development of Fracture Zones in Plain Concrete and Similar Materials*. Report No. TVBM-1006, Division of Building Materials, Lund Institute of Technology, Lund, Sweden.
- Planas, J., Guinea, G. V., and Elices, M. (1992). Stiffness associated with quasi-concentrate loads. *Materials and Structures*, 27:311–318.
- Reinhardt, H. W. (1981). Similitude of brittle fracture of structural concrete. In *Advanced Mechanics of Reinforced Concrete*, pages 175–184, Delf. IASBE Colloquium.
- RILEM/CEB/FIP (1970). Test and specifications of reinforcement for reinforced and pre-stressed concrete: Four recommendations of the RILEM/CEB/FIB,2: Pullout test. *Materials and Structures*, 3(15):175–178.
- Ruiz, G. (2001). Propagation of a cohesive crack crossing a reinforcement layer. *International Journal of Fracture*, 111(3):265–282.
- Ruiz, G. and Carmona, J. R. (2006). Experimental study on the influence of the shape of the cross-section and of the rebar arrangement on the fracture of lightly reinforced beams. *Materials and Structures*, 39:343–352.
- Ruiz, G., Elices, M., and Planas, J. (1998). Experimental study of fracture of lightly reinforced concrete beams. *Materials and Structures*, 31:683–691.